Earth and Planetary Science Letters 361 (2013) 208–218

Contents lists available at SciVerse ScienceDirect

Earth and Planetary Science Letters

journal homepage: www.elsevier.com/locate/epsl

Hot or not? Impact of seasonally variable soil carbonate formation on paleotemperature and O-isotope records from clumped isotope thermometry

Nathan A. Peters [a], Katharine W. Huntington [a,*], Gregory D. Hoke [b]

[a] Department of Earth and Space Sciences, University of Washington, Box 351310 Seattle, WA 98195-1310, USA
[b] Department of Earth Sciences, Heroy Geology Laboratory, Syracuse University, Syracuse, NY 13244, USA

ARTICLE INFO

Article history:
Received 9 July 2012
Received in revised form
26 October 2012
Accepted 26 October 2012
Editor: J. Lynch-Stieglitz
Available online 22 November 2012

Keywords:
pedogenic carbonate
clumped isotope thermometry
stable isotopes
paleoclimate
paleoaltimetry
temperature proxy

ABSTRACT

Quantifying the timing and temperature of soil carbonate formation is important for interpreting isotopic records of Earth-surface temperature and soil water composition from paleosols. Pedogenic carbonates typically have been assumed to form at mean annual temperature, but recent work suggests warm-season bias in carbonate formation could impact the interpretation of $\delta^{18}O$ values and carbonate formation temperatures for paleosol carbonates. We investigate the relationship between seasonally variable soil temperatures and carbonate formation temperatures estimated using clumped isotope thermometry ($T(\Delta_{47})$). Holocene soil carbonates were collected along the eastern flank of the Andes (33°S) over 2 km of relief and a nearly 15 °C range of mean annual air temperature (MAAT). This area receives both westerly, winter season precipitation and easterly, summer season precipitation, leading to a reversal of soil moisture regimes that occurs at ~2 km elevation. In instrumented pits sampled to 1 m depth, we do not observe systematic variation in $T(\Delta_{47})$ with depth or with elevation-dependent MAAT. Average $T(\Delta_{47})$ values for soil carbonates collected above 2 km elevation reflect summer soil temperatures. In contrast, $T(\Delta_{47})$ values below ~2 km track mean annual soil temperature. These results may reflect the dominance of summer precipitation below ~2 km, which likely delays soil drying and carbonate growth until fall. This seasonal variability in carbonate formation greatly impacts carbonate formation temperature, with important implications for estimating soil water $\delta^{18}O$ values. Calculating soil water $\delta^{18}O$ values using $T(\Delta_{47})$ produces a soil water $\delta^{18}O$ lapse rate of −4.6‰/km, remarkably similar to that of modern surface waters (−4.8‰/km), and significantly improving on previous soil water estimates assuming MAAT for carbonate formation temperatures. Although seasonal bias can prevent the straightforward translation of soil carbonate $T(\Delta_{47})$ into meaningful surface air temperatures, direct constraints on temperature from clumped isotopes can both provide a window into soil processes and aid in the interpretation of conventional stable isotopic data to reconstruct surface conditions in the past.

1. Introduction

Reconstructing past Earth-surface temperatures on continents is important for investigating the evolution of terrestrial environments, climate, tectonics, and landforms. A rich record of terrestrial paleoenvironments — and, potentially, of surface temperature — is archived in pedogenic carbonate. This carbonate, which forms in situ, is common in the geologic record, and the formation temperature and isotopic composition of the carbonate reflect a time average of the local, near-surface environmental conditions under which it forms (e.g. Quade et al., 1989a; Cerling and Quade, 1993; Breecker et al., 2009). The $\delta^{13}C$ and $\delta^{18}O$ values of soil carbonate have been used to investigate paleoenvironmental conditions such as atmospheric circulation and precipitation patterns (e.g. Amundson et al., 1996), climate-driven shifts in vegetation (e.g. Quade et al., 1989b; Cerling et al., 2011), and paleoaltimetry (e.g. Garzione et al., 2000; Rowley and Currie, 2006; Quade et al., 2007), but, until recently, it has been difficult to unambiguously determine paleotemperature from carbonate isotopic records. The difficulty arises because the carbonate $\delta^{18}O$ value depends on both the temperature of carbonate formation and $\delta^{18}O$ value of the water from which it forms (e.g. Kim and O'Neil, 1997), and estimating one of the two using carbonate $\delta^{18}O$ values alone requires an assumption about the other.

Clumped isotope thermometry (Ghosh et al., 2006a; Eiler, 2007) alleviates this problem by independently constraining both the formation temperature and $\delta^{18}O$ value of carbonate. While several recent studies have used clumped isotopes to determine the formation temperature of paleosol carbonates (Ghosh et al., 2006b; Passey et al., 2010; Quade et al., 2007, 2011), it is not

* Corresponding author. Tel.: +1 206 543 1750.
E-mail address: kate1@uw.edu (K.W. Huntington).

0012-821X/$ - see front matter © 2012 Elsevier B.V. All rights reserved.
http://dx.doi.org/10.1016/j.epsl.2012.10.024

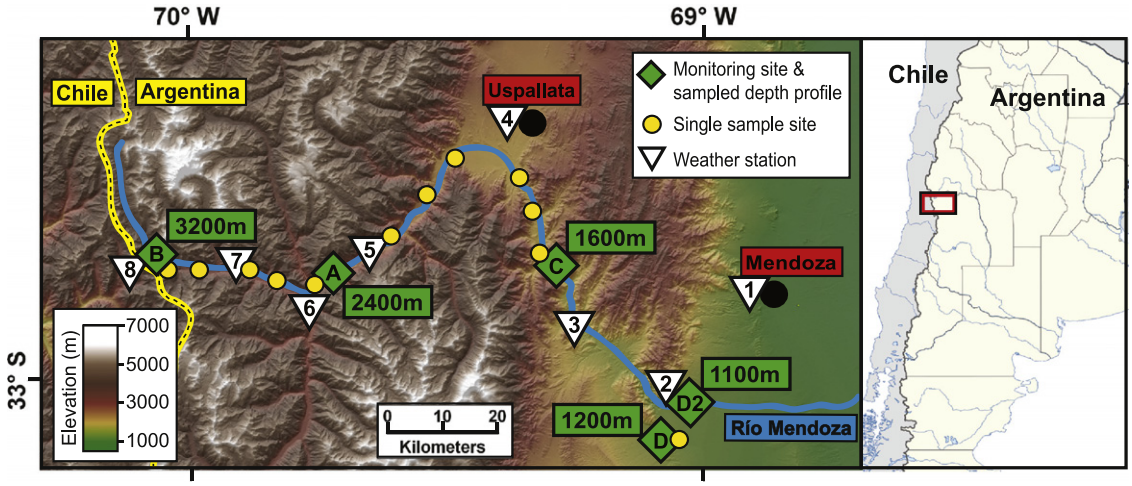

Fig. 1. Shaded relief map showing the study region in Argentina with approximate locations for monitoring sites (green diamonds—with site labels), sites of single ~50–60 cm depth samples (yellow circles), and weather stations (white triangles—with station numbers). Station 1, Mendoza; 2, Cacheuta; 3, Guido; 4, Uspallata; 5, Polveredas; 6, Punta de Vacas; 7, Puente del Inca; 8, Las Cuevas. (For interpretation of the references to color in this figure legend, the reader is referred to the web version of this article.)

known how such temperatures relate to actual air and soil temperatures at Earth's surface (e.g. Retallack, 2009; Sheldon and Tabor, 2009; Eiler, 2011). Carbonate formation temperature in paleoenvironmental studies is generally assumed to reflect mean-annual air temperature (MAAT) (e.g. Cerling and Quade, 1993; Quade et al., 1989a, 2007). However, recent work suggests a strong seasonal bias in pedogenic carbonate formation that would invalidate this assumption (Breecker et al., 2009; Passey et al., 2010; Quade et al., 2011) and impact the way both carbonate $\delta^{18}O$ and temperature records are interpreted. Thus the challenge lies in constraining not only the temperature of carbonate formation, but also the relationships between the formation temperature and isotopic composition of carbonate, soil subsurface conditions, and aboveground environment.

In this study, we compare measured subsurface soil and local air temperature to direct estimates of carbonate formation temperatures from clumped-isotope thermometry of Holocene soils collected in the southern Central Andes of Argentina (~33°S; Fig. 1). This region spans over 2 km of relief, exhibits variable seasonality of precipitation, samples a wide range of temperatures, and was the site of previous work documenting the elevation dependence of $\delta^{18}O$ values in precipitation, river water, and pedogenic carbonate (Hoke et al., 2009, 2011). Our goals are to (1) tease apart the influence of seasonal precipitation, air temperature, and soil temperature on temperatures of soil carbonate formation as determined by clumped isotope thermometry and (2) determine how well clumped-isotope temperatures ($T(\Delta_{47})$) for Holocene soil carbonates and calculated soil water $\delta^{18}O$ values predict modern elevation and the isotopic composition of modern surface waters. To this end, we infer the season of carbonate formation at each sample site by placing the $T(\Delta_{47})$ data in the context of relevant environmental factors such as season of precipitation, elevation, and vegetation. Our results have broad applicability to interpreting estimates of soil carbonate formation temperature from clumped isotope thermometry and improving reconstructions of soil water $\delta^{18}O$ values from pedogenic carbonates.

2. Pedogenic carbonate formation

Pedogenic carbonate (typically calcite, $CaCO_3$) commonly forms in strongly seasonal arid to sub-humid environments through dissolution–precipitation reactions in the soil. Over hundreds to thousands of years, carbonate accumulates in the soil profile (Gile et al., 1966; Birkeland, 1999). The Ca^{2+} ions required for carbonate accumulation are provided by rainwater and dissolution of Ca-bearing minerals in soil parent material or transported dust (Monger and Wilding, 2006). Carbon in pedogenic carbonates is derived primarily from soil CO_2 produced by plant root and microbial respiration, which is depleted in ^{13}C relative to atmospheric CO_2; contributions from atmospheric CO_2 lead to a positive shift in soil carbonate $\delta^{13}C$ values near the surface (Cerling and Quade, 1993). Oxygen in pedogenic carbonate is derived from soil water, and the $\delta^{18}O$ value of the carbonate depends on the $\delta^{18}O$ value of the soil water and temperature-dependent oxygen-isotope fractionation during carbonate formation (e.g. Kim and O'Neil, 1997). In well-drained soils, precipitation is the primary source of soil water. The $\delta^{18}O$ of rainwater or snow depends on factors including temperature, latitude, amount, continentality, and elevation, (e.g. Rowley et al., 2001; Gonfiantini et al., 2001), and water near the surface in a soil profile (depths of <40 cm) is generally evaporatively enriched in ^{18}O with respect to ^{16}O.

Carbonate precipitation and dissolution reactions are influenced by changes in soil moisture, temperature, and pCO_2 that vary interannually, seasonally, and daily (e.g. Wood and Petraitis, 1984; Flanagan and Varney, 1995; Flerchinger and Pierson, 1997; Austin et al., 2004; Retallack, 2005), influencing the temperature and $\delta^{18}O$ value of soil waters at the time of carbonate growth (Cerling and Quade, 1993). Carbonate forms when soil water loss and CO_2 degassing cause the soil solution to become supersaturated with respect to calcium carbonate. Breecker et al. (2009) monitored seasonal changes in soil chemistry in New Mexico and found that supersaturation was favored during warm, dry periods, when calcite solubility was lowest and C and O isotopic equilibrium were reached. This finding suggests soil carbonate formation does not reflect mean annual or mean growing season conditions as is typically assumed, impacting the temperature and $\delta^{18}O$ values recorded by soil carbonates. Indeed, recent clumped isotope studies suggest that carbonate formation temperatures are hotter than MAAT and may be closer to or even above warmest monthly mean air temperatures due to radiative solar heating of the ground surface (e.g. Coops et al., 2000, Bartlett et al., 2006) and timing of carbonate formation (Passey et al., 2010; Quade et al., 2011), regardless of soil moisture regime (Quade et al., in press). Given that seasonal variations in temperature and the $\delta^{18}O$ value of precipitation at the same site can

vary by 30 °C and 20‰, respectively (e.g. Gonfiantini et al., 2001; Hoke et al., 2011), testing this hypothesis is critical if we are to interpret paleosol temperature and isotopic records correctly.

3. Background: study region

Our approach is to investigate Holocene soil carbonates along an elevation transect that exhibits a wide range of MAAT and soil water regimes. Our target soils must be young (Holocene) to ensure our modern climate observations approximate the conditions under which the soil carbonate samples formed. Because soil temperature varies with depth, the soils must be developed in parent material that has not experienced significant aggradation or erosion during carbonate formation. The Río Mendoza valley, Argentina, exhibits opposite seasonality of precipitation and a wide range of MAAT over a small distance and hosts Holocene terrace deposits with abundant soil carbonate, making it an ideal location for our study.

3.1. Geographic setting and chronology

The Río Mendoza valley (Fig. 1) is located at ~33°S latitude in the southern Central Andes, Argentina. The ~100 km long, roughly east–west transect spans over 2 km of relief along Argentine National Route 7 and is the site of previous work by Hoke et al. (2009), who targeted unconsolidated terrace deposits with early stage carbonate formation. The physiographic provinces of the Andes along the sampling transect include from east to west the Precordillera foothills, Frontal Cordillera, Uspallata Valley, and Principal Cordillera (Jordan et al., 1983; Cristallini and Ramos, 2000).

The chronology of glacial deposits in the Frontal and Principal Cordilleras places constraints on the age of the soil carbonates in the Río Mendoza valley. The oldest and lowest known glacial moraine is the middle Pleistocene Uspallata Moraine, which is located at an elevation of 1850 m (Espizúa and Bigazzi, 1998). Subsequent Late Pleistocene glacial deposits include, from oldest to youngest, the Punta de Vacas, Penitentes, Horcones, and Almacenes drifts. While the Penitentes glacial advance occurred before ca. 40 kya, prior to the last glacial maximum, the Horcones and Almacenes drifts document glaciation in the upper portion of the valley after 15 kya (Espizúa, 1999), and perhaps as recently as 11–10 kya (Espizúa, 2002, 2003). The Horcones drift deposits extend to 2650 m near Puente del Inca (Fig. 1) and are characterized by incipient soil development and clasts with discontinuous carbonate coatings (stage I, Gile et al., 1966). Outwash terrace deposits associated with the Horcones drift extend east of the terminal moraine 10–20 m above the Río de las Cuevas and Río Mendoza. Although the Precordillera shows no evidence of having been glaciated, downstream of Uspallata the sediments deposited in the Río Mendoza valley are dominated by glacial outwash and are mapped as postglacial (Polanski, 1963). Thus we can be confident that soil carbonates developed in deposits overlying the Horcones and Almacenes drifts or in the youngest glacial outwash terraces are Holocene, making it appropriate to examine their formation temperatures in the context of modern climate.

3.2. Regional climatic setting

Due to its semi-arid climate and high relief, the Río Mendoza valley exhibits a range of MAAT as well as large seasonal variations in temperature. MAAT decreases with elevation at a rate of ~6 °C/km (Hoke et al., 2009), resulting in a nearly 15 °C range of MAAT along our 100 km transect. Seasonal temperature differences are even greater, with winter and summer average temperatures differing by up to 17 °C. These large variations make this an excellent locale to explore how the temperature of pedogenic carbonate formation relates to seasonal variations in air and soil temperatures well outside the ~2 °C uncertainty in $T(\Delta_{47})$.

The source and seasonality of precipitation also vary across the study area due to the influence of the Andes on atmospheric circulation. During austral winter (JJA), weakening and northward displacement of the subtropical Pacific anticyclone enhances westerly flow across the Andes (Saavedra and Foppiano, 1992). Between 30°S and 37°S, the Andes influence this flow, significantly blocking moisture transport from the Pacific Ocean (Viale and Nuñez, 2011); however, winter precipitation does cross the continental divide into the study area (Fig. 1; Hoke et al., 2011). In austral summer (DJF), the interaction of semi-permanent low pressure in Argentina and the subtropical South Atlantic anticyclone generates northeasterly flow over central regions of Argentina, causing net moisture transport to the eastern slopes of the Andes (Barros et al., 1996). The result is that the upper portion of the valley (west of Uspallata) receives the majority of its precipitation during the winter (primarily as snow), and the lower portion (east of Uspallata) receives the majority of its precipitation in the summer. By exploiting this seasonal variation in precipitation source and amount over a range of elevations, we can investigate how formation temperatures and $\delta^{18}O$ values of carbonate vary as a function of precipitation regime as well as temperature.

4. Methods

4.1. Site selection and sampling

Soil carbonate samples were collected along the Río Mendoza valley from soil pits and from trenches excavated on the banks of Holocene glacial outwash terrace deposits and, in a few cases, landslide deposits (Polanski, 1963; Pereyra, 1996; Espizúa, 1999; Moreiras, 2010, 2011). In January 2010, we excavated four soil pits to depths of ~1 m at elevations of ~1200, 1600, 2400 and 3200 m (Fig. 1). In January 2011, we excavated a fifth ~1 m-deep soil pit at ~1100 m. The 3200 m site is located on the Cristo Redentor rotational slide (Pereyra, 1996), and the four lower elevation sites are located in the lowest (youngest) of a series of clast rich alluvial terraces created by the incising Río Mendoza as it reworked post-glacial outwash deposits (Table 1). We sampled soil carbonate from depth profiles with 5–20 cm spacing from the uppermost occurrence of carbonate to the bottom of each pit. Additional samples were collected at 50–60 cm depths from smaller soil pits and trenched soil profile exposures dug into these young terraces at intermediate elevations in 2007 and 2011; the samples collected in 2007 are separates of the samples analyzed by Hoke et al. (2009) (MODS samples, Table 3).

The youngest possible carbonates were sampled based on incipient soil development and carbonate morphology. We selected non-carbonate clasts with carbonate coatings found only on the underside of the clasts to ensure that the carbonate formed in-situ, and we avoided profiles with coatings in random orientations suggestive of post-depositional reworking. In the field, we used criteria to infer surface stability following initiation of soil development, including presence of uniform parent material and lack of anthropogenic modification, erosion, or deposition as indicated by vegetation, desert pavement, weathering, and lack of buried soil horizons. Carbonate $\delta^{18}O$ and $\delta^{13}C$ depth profiles were analyzed to evaluate soil profile disturbance (see Section 5.2).

Table 1
Weather station summary.

Station[a]	Location	Elevation	Position[b]		Data available[c]	Data source[c]
#		(m)	Latitude (S)	Longitude (W)	(years)	
1	Mendoza	800	32° 54.98′	68° 50.68′	Air T, precip. (1981–1990)	SMN
2	Cacheuta	1200	33° 0.90′	69° 7.05′	Precip. (1983–2012)	DRH
3	Guido	1400	32° 54.96′	69° 14.23′	Air T (1965–2012), precip. (1957–2012)	DRH
4	Uspallata	1900	32° 35.67′	69° 20.38′	Air T (1993–2012), precip. (1983–2012)	DRH
5	Polvaredas	2200	32° 47.68′	69° 39.28′	Precip. (1983–2012)	DRH
6	Punta de Vacas	2400	32° 51.35′	69° 45.68′	Air T (1992–2012), precip. (1992–2012)	DRH
7	Puente del Inca	2700	32° 49.46′	69° 54.68′	Air T, precip (1971–1976)	SMN
8	Cristo Redentor	3800	32° 49.51′	70° 4.27′	Air T (1971–1980)	SMN

[a] Station numbers correspond to numbers in Figs. 1, 3, 5, and A1.
[b] Station positions are approximated due to innacurate coordinates reported by Dirección de Recursos Hídricos (DRH).
[c] Weather data from DRH include daily total precipitation for all stations and daily minimum and maximum air temperature for some stations. Data from Servicio Metereológico Nacional (SMN) include monthly mean air temperature and monthly mean total precipitation.

Table 2
Summary of sample sites.

Site	Elevation	Location		Sample depth	Carbonate morphology[a]
	(m)	Latitude (S)	Longitude (W)	(cm)	
1100 m monitoring site (D2)[b]	1090	33° 2.635′	69° 0.553′	15-100	II
1200 m monitoring site (D)[b]	1170	33° 4.850′	69° 2.768′	20–100	I
RM1333-11	1330	33° 5.442′	69° 6.021′	60	Early I
MODS 07-03	1600	32° 48.840′	69° 18.060′	~50	I
1600 m monitoring site (C)[b]	1600	32° 49.401′	69° 17.915′	10–100	I/II
RM1695-11	1700	32° 43.807′	69° 19.697′	60	Early I
RM1947-11	1950	32° 38.437′	69° 29.946′	60	Early I
MODS 07-05	2000	32° 39.720′	69° 30.780′	~50	I
MODS 07-06	2200	32° 46.140′	69° 35.880′	~50	I
2400 m monitoring site (A)[b]	2350	32° 50.090′	69° 43.715′	10–100	I
MODS 07-07	2400	32° 50.520′	69° 44.640′	~50	I
MODS 07-10	2600	32° 50.700′	69° 49.620′	~50	I
MODS 07-08b	3200	32° 48.720′	70° 3.720′	~50	I
3200 m monitoring site (B)[b]	3220	32° 48.709′	70° 3.868′	15–100	Early I

[a] Carbonate morphologies defined by Gile et al. (1966).
[b] Study site letter designations correspond to those in Fig. 1.

4.2. Monitoring of subsurface conditions and local weather

To characterize seasonal variations in soil subsurface conditions, we installed Onset HOBO microstation data loggers (model H21-002) at each of the monitoring sites. Temperature sensors (S-TMB-M002) were placed at depths of 10, 50, and 100 cm. Soil moisture sensors (S-SMC-M005) were placed at 50 cm depth, but since the soil moisture sensor values were correlated with soil temperature and did not show increases in soil moisture coincident with known precipitation events, the data are not discussed further. The influence of soil disturbance during pit excavation was minimized by inserting sensor probes 10–20 cm into the pit wall and by delaying the start of monitoring until one month after sensor installation and pit refilling. Air temperature at each of the depth-profile sites was measured with HOBO UA-001-64 pendent loggers installed within radiation shields 1.0–1.2 m above the ground surface (Fig. 2). Subsurface and air temperature data were sampled every 15 min from February 2010 to February 2011. In January 2011, monitoring equipment from the 1200 m site was removed and reinstalled at the 1100 m site. The relocation of the 1200 m station was motivated by preliminary isotopic analyses, which revealed that carbonate samples from the 1200 m pit contained contaminants that produced spurious clumped isotope results (Section 5.2). Both the 1100 and 1200 m monitoring sites are located on flat river terraces in open terrain with similar vegetation species and density.

In addition to collecting onsite monitoring data, we obtained weather station daily air temperature and precipitation data from the Dirección de Recursos Hídricos, a data clearinghouse for several national and provincial agencies in Argentina (http://www.hidricosargentina.gov.ar), and additional monthly mean weather data were obtained from Servicio Meteorológco Naciónal (http://www.smn.gov.ar) (Table 2; Fig. 1). These data place our local site monitoring data in the context of longer-term weather trends in the region. Historical weather records in this region go as far back as 1957, but individual stations record weather data over different time intervals (Table 2).

4.3. Isotopic analysis

In preparation for isotopic analysis (Δ_{47}, $\delta^{18}O$, $\delta^{13}C$), carbonate coatings on clasts were lightly brushed with a toothbrush to remove small roots and sediment particles. The carbonate was scraped from the clast using a razor blade and gently powdered in an agate mortar. Most samples include carbonate coatings from multiple clasts collected from the same depth, mixed to homogenize carbonate. To evaluate the variability in the Δ_{47}, $\delta^{18}O$, and $\delta^{13}C$ values of carbonate from neighboring clasts at the same depth, carbonate from individual clasts at 75 cm depth from the

Table 3
Summary of isotopic analyses for carbonate samples along the transect.

Sample	*n*	Elevation (m)	Depth (cm)	$\delta^{13}C$[a] (‰, VPDB)	$\delta^{18}O$[a] (‰, VPDB)	Δ_{47} ±1SE[a] (‰)	T(Δ_{47}) ±1SE (°C)	Soil water $\delta^{18}O$[b] (‰, VSMOW)
1100 m monitoring site (D2)								
D2-20	2	1090	20	−3.23	−1.093	0.654 ± 0.013[c]	23 ± 3	0.9 ± 0.6
D2-50	3	1090	50	−5.85	−1.223	0.686 ± 0.021	17 ± 4	−0.5 ± 0.8
D2-80	1	1090	80	−4.61	−3.818	0.686 ± 0.037[d]	16 ± 6	−3.3 ± 1.0
D2-100	3	1090	100	−4.86	−3.041	0.640 ± 0.010[c]	26 ± 2	−0.5 ± 0.4
RM1333-11-60	2	1330	60	−5.25	−11.408	0.664 ± 0.013[c]	21 ± 3	−9.9 ± 0.6
MODS 07-03	3	1600	~50	−5.80	−7.727	0.683 ± 0.020	17 ± 4	−7.0 ± 0.8
1600m monitoring site (C)								
C10	3	1600	10	−2.27	−3.656	0.673 ± 0.010[c]	19 ± 2	−2.5 ± 0.4
C35	2	1600	35	−3.87	−8.284	0.652 ± 0.013[c]	24 ± 3	−6.1 ± 0.6
C47	2	1600	47	−4.94	−9.506	0.647 ± 0.013[c]	25 ± 3	−7.1 ± 0.6
C50	2	1600	50	−5.52	−9.720	0.688 ± 0.013[c]	16 ± 3	−9.2 ± 0.6
C85	2	1600	85	−5.69	−10.874	0.664 ± 0.013[c]	21 ± 3	−9.3 ± 0.6
C100	2	1600	100	−6.77	−10.952	0.672 ± 0.013[c]	19 ± 3	−9.8 ± 0.6
RM1695-11-60	3	1700	60	−4.20	−11.728	0.671 ± 0.012	19 ± 3	−10.6 ± 0.6
RM1947-11-60	2	1950	60	−6.30	−12.346	0.663 ± 0.015	21 ± 3	−10.8 ± 0.6
MODS 07-05	2	2000	~50	−2.80	−7.312	0.683 ± 0.033	17 ± 5	−6.6 ± 1.0
MODS 07-06	2	2200	~50	−3.66	−14.434	0.640 ± 0.007[c]	27 ± 2	−11.7 ± 0.4
2400m monitoring site (A)								
A10	2	2350	10	−0.93	−11.333	0.662 ± 0.013[c]	21 ± 3	−9.8 ± 0.6
A20	2	2350	20	−3.06	−13.422	0.644 ± 0.022	25 ± 4	−11.1 ± 0.8
A30	2	2350	30	−4.20	−15.085	0.672 ± 0.013[c]	19 ± 3	−14.0 ± 0.6
A50	4	2350	50	−4.59	−15.922	0.659 ± 0.009[c]	22 ± 2	−14.2 ± 0.4
A75A	2	2350	75	−4.64	−15.954	0.664 ± 0.036	21 ± 6	−14.4 ± 1.2
A75B	3	2350	75	−5.67	−16.049	0.651 ± 0.010[c]	24 ± 2	−13.9 ± 0.4
A901	2	2350	90	−4.98	−15.497	0.659 ± 0.021	22 ± 4	−13.8 ± 0.8
A902	3	2350	90	−4.44	−15.594	0.661 ± 0.021	22 ± 4	−13.9 ± 0.8
A100U	4	2350	100	−5.44	−15.418	0.653 ± 0.009[c]	23 ± 2	−13.5 ± 0.4
MODS 07-07	2	2400	~50	−5.61	−15.413	0.662 ± 0.015	21 ± 3	−13.9 ± 0.6
MODS 07-10	2	2600	~50	1.25	−16.061	0.660 ± 0.007	22 ± 2	−14.3 ± 0.4
3200m monitoring site (B)								
B15	4	3220	15	−2.08	−10.664	0.684 ± 0.010[c]	17 ± 2	−10.0 ± 0.4
B30	2	3220	30	−5.37	−11.828	0.675 ± 0.021	19 ± 4	−10.7 ± 0.8
B45	4	3220	45	−4.67	−12.839	0.711 ± 0.009[c]	11 ± 2	−13.4 ± 0.4
B65	2	3220	65	−2.61	−11.865	0.702 ± 0.013[c]	13 ± 3	−12.0 ± 0.6
B80	2	3220	80	−5.75	−14.117	0.667 ± 0.018	21 ± 4	−12.6 ± 0.8
B100	2	3220	100	−6.85	−14.690	0.687 ± 0.013[c]	16 ± 3	−14.2 ± 0.6
MODS 07-08b	3	3200	~50	−6.87	−15.568	0.688 ± 0.030	16 ± 6	−15.1 ± 1.0

[a] Carbonate $\delta^{13}C$, $\delta^{18}O$ reported as mean and Δ_{47} reported as weighted mean of replicates (*n*) for each individual sample. Average external error (1SE) for replicates of a sample is ±0.04‰ for $\delta^{13}C$, ±0.002‰ for $\delta^{18}O$, and ±0.016‰ for Δ_{47}.

[b] Soil water $\delta^{18}O$ was calculated using the calcite–water O-isotope fractionation equation of Kim and O'Neil (1997). Uncertainty in soil water $\delta^{18}O$ was calculated by propagating errors in $T(\Delta_{47})$.

[c] For samples with fortuitously low SE for replicates, SE was assigned using the long-term SD of a standard run during the same period of time divided by sqrt(*n*), where *n* is the number of sample replicates; uncertainty for 95I123 from Huntington et al. (2009) (S.D.=0.009‰) was used for MODS samples and Carrara marble (S.D.=0.018‰) was used for all other samples.

[d] Unreplicated sample error is SE of eight acquisitions for a single analysis.

2400 m site (A75A and A75B) and 47–50 cm depth from the 1600 m site (C47 and C50) was analyzed separately rather than being homogenized. Additionally, two discrete layers of carbonate rind on a clast from 90 cm depth at the 2400 m site were sampled for separate analysis (A901 and A902).

Isotopic analyses were conducted at the California Institute of Technology. Samples collected in 2007 (MODS samples, Table 3) were digested in anhydrous phosphoric acid at 25 °C, and resulting CO_2 was purified using the apparatus described by Ghosh et al. (2006a) and methods of Huntington et al. (2010). Samples collected in 2010 and 2011 were digested at 90 °C, and CO_2 was purified using methods described by Passey et al. (2010). The CO_2 was analyzed on a ThermoFinnigan MAT 253 mass spectrometer configured to measure masses 44–49 inclusive (e.g. Eiler and Schauble, 2004). Measured Δ_{47} values were normalized for stretching and nonlinearity following Huntington et al. (2009). Two to five external replicate analyses were conducted for each sample. Mass-48 values were used to screen for contaminants (e.g. Eiler and Schauble, 2004; Huntington et al., 2009), and samples with mass-48 values exceeding the values measured for clean, heated CO_2 gases by >1‰ were rejected. Carbonate $\delta^{18}O$ and $\delta^{13}C$ values were referenced to VSMOW and VPDB. International and in-house carbonate Δ_{47} standards were analyzed along with the samples; Carmel chalk (accepted Δ_{47} value 0.644‰) yielded an average value of 0.652 ± 0.020‰, Carrara marble (accepted Δ_{47} value 0.352‰) yielded an average value of 0.345 ± 0.018‰ and TV01 (accepted Δ_{47} value 0.662‰) yielded an average of 0.669 ± 0.018‰ (all 1 standard deviation). Calcite

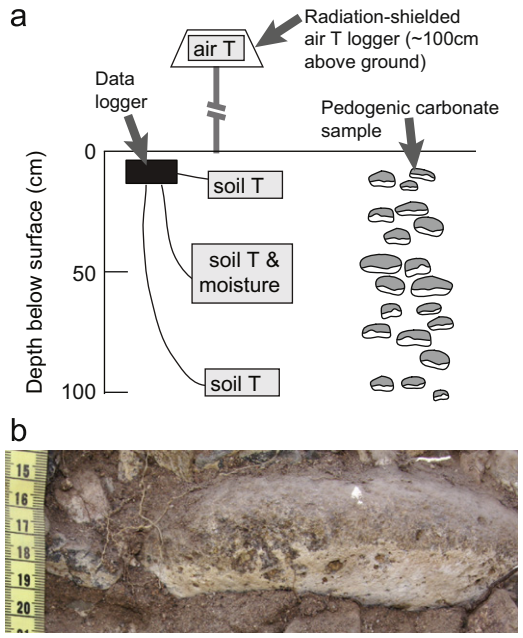

Fig. 2. (a) Schematic diagram of monitoring site setup and sampling strategy showing placement of temperature and soil moisture sensors (gray boxes). For each monitoring site, clasts with carbonate pendants (undercoatings) were sampled at 5–20 cm vertical spacing to a depth of ~100 cm. (b) Example of a carbonate sample taken from the 1600 m monitoring site exhibiting late stage I to stage II carbonate pendants.

formation temperatures were calculated from Δ_{47} values using the Ghosh et al. (2006) calibration and temperature errors were calculated after Huntington et al. (2009). Soil water $\delta^{18}O$ values were calculated from measured T(Δ_{47}) and $\delta^{18}O$ values of calcite using the calcite-water fractionation relation of Kim and O'Neil (1997).

5. Results

5.1. Temperature and precipitation monitoring data

Decadal-scale air temperatures are constrained by permanent weather stations along the sample transect. MAAT decreases with elevation from 17 °C at 800 m to −1.6 °C at 3800 m, and, based on a linear regression of MAAT for all weather stations along the transect, the lapse rate is −5.9 °C/km (r^2=0.94). Seasonal variations in monthly mean air temperature at a given station range from 17 °C at 800 m to 11 °C at 3800 m, reflecting the general decrease in the difference between warmest average monthly air temperature (WAMT) and coldest average monthly air temperature with elevation. Nearby weather station data show that our in-situ monitoring sites experienced monthly mean air temperatures for summer (DJF) of 2009–2010 that were 1–2 °C higher than the historical average over those months, summer 2010–2011 air temperatures within 1 °C of historical averages, and mean winter (JJA) temperatures 0–4 °C below average; however, these values are all within 2σ of the historical averages. The weather station data are complemented by site-specific information from pendant air temperature data loggers at each soil-monitoring site. All of our monitoring and sampling sites are within 8 km of meteorological stations. Two of the air temperature sensors (3200 m and 2400 m) recorded data over the duration of the 2010–2011 soil-monitoring period. We compared the temperature data from the closest monitoring site-weather station pair (2400 m and Punta de Vacas) and found MAAT values to be within 0.5 °C, demonstrating that weather station MAAT is representative of conditions at our sample sites. We were unable to obtain useful data from the 1200 m logger (detached from pole) or the 1600 m logger (missing).

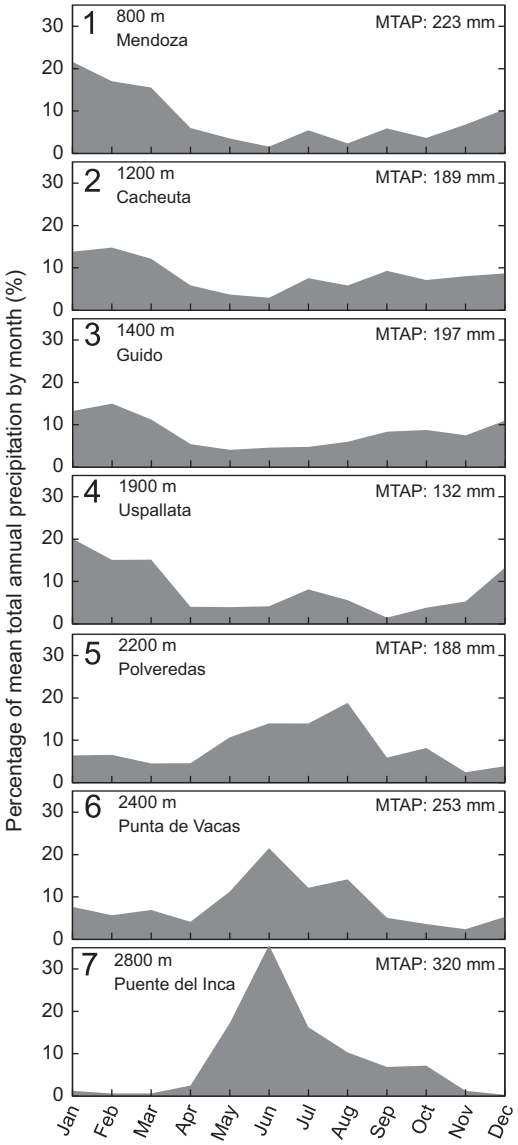

Fig. 3. Monthly percentages of mean total annual precipitation (MTAP) for all weather stations along the transect. For stations at 800–1900 m elevations (1–4), 37–49% of total precipitation occurs in the summer months (DJF). For stations at 2200–2800 m elevations (5–7), 47–62% of total precipitation occurs in the winter months (JJA). See Fig. 1 for weather station locations along the transect.

Mean annual soil temperature (MAST) along the transect decreases systematically with elevation at an average rate of −5.4 °C/km (r^2=0.89), which is 0.5 °C/km lower than that observed for MAAT. MAST measured from monitoring sites is 3.5–5.0 °C above MAAT, as interpolated from nearby weather stations. MAST is the same at 10, 50, and 100 cm depths for all four monitoring sites within the error of the temperature probes (±0.3 °C). Daily variation in soil temperatures is greatest in the summer, when the effect of solar heating of the surface is greatest. Near the surface (10 cm), daily variation can be as great as 14 °C, with maximum temperatures occurring in the evening, generally around 7 pm. Daily variation at 50 cm depth is considerably dampened (<2 °C) and out of phase with surface temperatures. At 50 cm depth, maximum temperatures generally occur around 1 am. At 100 cm depth, daily temperature cycles are completely dampened out.

The amount and seasonality of precipitation vary across the region as a function of elevation (Fig. 3; Fig. A1 in the Electronic Appendix). Whereas at the lowest elevation stations precipitation is concentrated in the summer half of the year, at high elevation precipitation is concentrated in winter. At intermediate elevations (near Uspallata, 1900 m), a mix of both winter and summer precipitation is observed. Weather station precipitation data are used to infer seasonal trends in soil moisture conditions.

5.2. Isotopic data

Results from clumped isotope analyses, including $\delta^{18}O$, $\delta^{13}C$, and $T(\Delta_{47})$ values, are summarized in Table 3 and Figs. 4 and 5 (details in the Electronic Appendix Table A1). The Δ_{47} results for samples from the 1200 m site showed signs of contamination as indicated by anomalous mass-48 values and are not discussed further. Depth profiles of $\delta^{18}O$ and $\delta^{13}C$ from the 1100, 1600, 2400, and 3200 m sites show constant values below ~50 cm and enrichment toward the soil surface (Fig. 4), confirming that they are undisturbed soil profiles. Values of carbonate $\delta^{18}O$ for single samples at 50–65 cm depth and means for monitoring site depth profile samples below 60 cm decrease from −3.4‰ at 1100 m to −15.6‰ at 3200 m, with the lowest value along the transect of −16.1‰ occurring at 2600 m (MODS 07-10). Carbonate $\delta^{13}C$ values range from −6.87‰ to 1.25‰, but mean values of carbonate $\delta^{13}C$ for depth profile samples below 50 cm are all between −6 and −5‰ and do not vary significantly with elevation, reflecting dominantly C_3 vegetation (Cavagnaro, 1988) and low overall productivity (Cerling and Quade, 1993). Values of Δ_{47} for all samples range from 0.640‰ to 0.711‰, with external precision (1SE for all replicates of a sample) varying from 0.007‰ to 0.037‰. The range of Δ_{47} values translates to carbonate formation temperatures of 11–26 °C, with external errors in $T(\Delta_{47})$ averaging 3 °C and ranging from ±2 to ±6 °C (Fig. 4). Although $T(\Delta_{47})$ values for two samples from separate clasts at the same depth (A75A and A75B; 2400 m monitoring site) agree within 1SE, $T(\Delta_{47})$ values for samples collected at similar depths (C47 and C50; 2400 m monitoring site) differ by 9 °C ($T(\Delta_{47})$ errors of ±3 °C on both samples). Samples from two discrete layers on the same clast (A901 and A902; 2400 m monitoring site) are indistinguishable. The amount by which mean $T(\Delta_{47})$ values for monitoring site profiles exceed MAST increases from 2 °C above MAST at 1100 m to 9 °C above MAST at the 3200 m site (Fig. 4). Soil water $\delta^{18}O$ values calculated from measured carbonate $\delta^{18}O$ and $T(\Delta_{47})$ values decreases with elevation at a rate of −4.6‰/km.

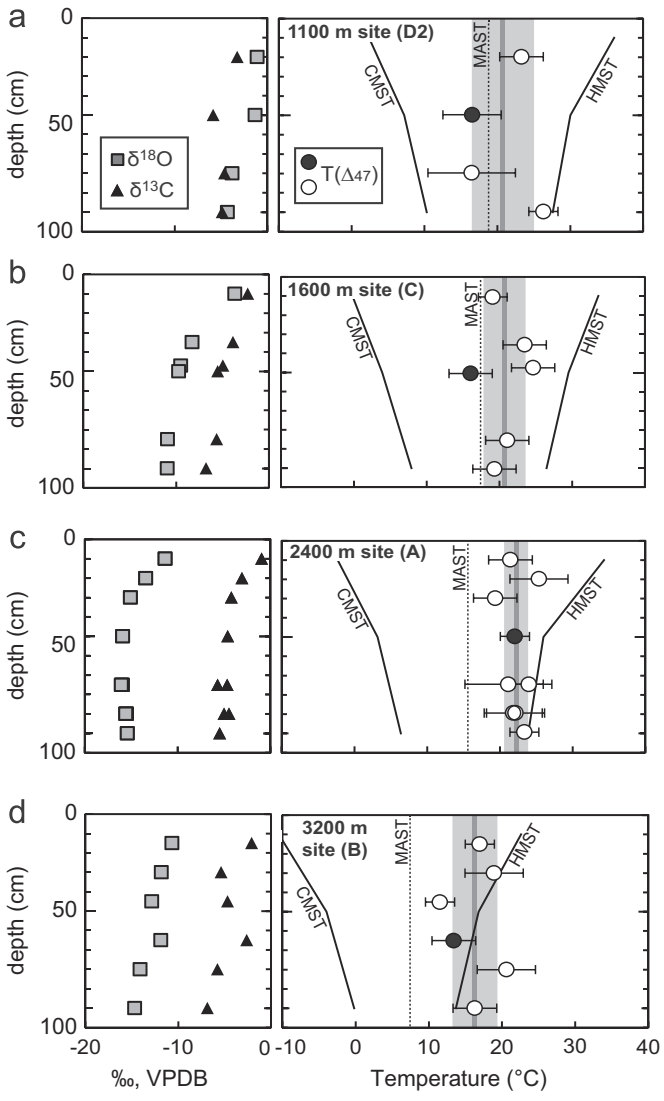

Fig. 4. Depth profiles of carbonate $\delta^{18}O$ and $\delta^{13}C$ values (VPDB) and $T(\Delta_{47})$ for samples from monitoring sites along the transect. *Left panels:* depth profiles of carbonate $\delta^{18}O$ (gray boxes) and $\delta^{13}C$ (black triangles) show approximately constant values below ~50 cm and enrichment toward the surface. *Right panels*: depth profiles of $T(\Delta_{47})$ for soil carbonate samples and soil temperatures measured Dec 2010–Feb 2011 at depths of 10, 50, and 100 cm, including: coldest measured soil temperature (CMST; solid line), mean annual soil temperature (MAST; vertical dashed line), and hottest measured soil temperature (HMST; solid line). Black circles are single samples closest to 60 cm depth (50–65 cm), and open circles are all samples from other depths (average $T(\Delta_{47})$ values for replicates; error bars are 1SE). Gray vertical lines and shaded boxes indicate the mean and standard deviation of all $T(\Delta_{47})$ values in a profile, respectively.

6. Discussion

Previous work suggests pedogenic carbonate should form in equilibrium during the warm season; thus we expected our $T(\Delta_{47})$ results to (1) reflect summer soil temperature profiles (i.e., WAMT near the surface and decreasing temperature with depth), and (2) systematically decrease with elevation. Average $T(\Delta_{47})$ values for samples above ~2000 m elevation approach WAMT and are generally consistent with these expectations. However, $T(\Delta_{47})$ values for samples <2000 m do not. Lower-elevation samples are closer to MAAT, and the result is that carbonate growth temperatures for the 1100 m and 3200 m samples are indistinguishable. We also do not observe systematic trends in $T(\Delta_{47})$ with depth. The following paragraphs detail these trends and explore possible explanations for why our observations are not consistent with warm season soil carbonate formation everywhere.

6.1. Soil carbonate $T(\Delta_{47})$ vs. air and soil temperature

We expect that $T(\Delta_{47})$ would record warm season soil temperatures, which should fall between MAAT and WAMT, or be warmer if solar heating of soil raises soil temperatures significantly over air temperatures. Our in-situ monitoring and weather station data show that MAAT, WAMT, and soil temperatures decrease systematically with elevation, bracketing the range of expected soil carbonate $T(\Delta_{47})$ values. Fig. 5 compares measured air and soil temperatures to $T(\Delta_{47})$ results for all sampled locations, including data for single samples collected at 50–65 cm and for multiple samples collected from various depths in the monitoring pits (Fig. 4). Although average $T(\Delta_{47})$ values are generally between MAAT and WAMT, mean $T(\Delta_{47})$ values for a given pit profile increase from 5 °C above MAAT at the 1100 m site to 12 °C above MAAT at the 3200 m site. Thus while $T(\Delta_{47})$ results

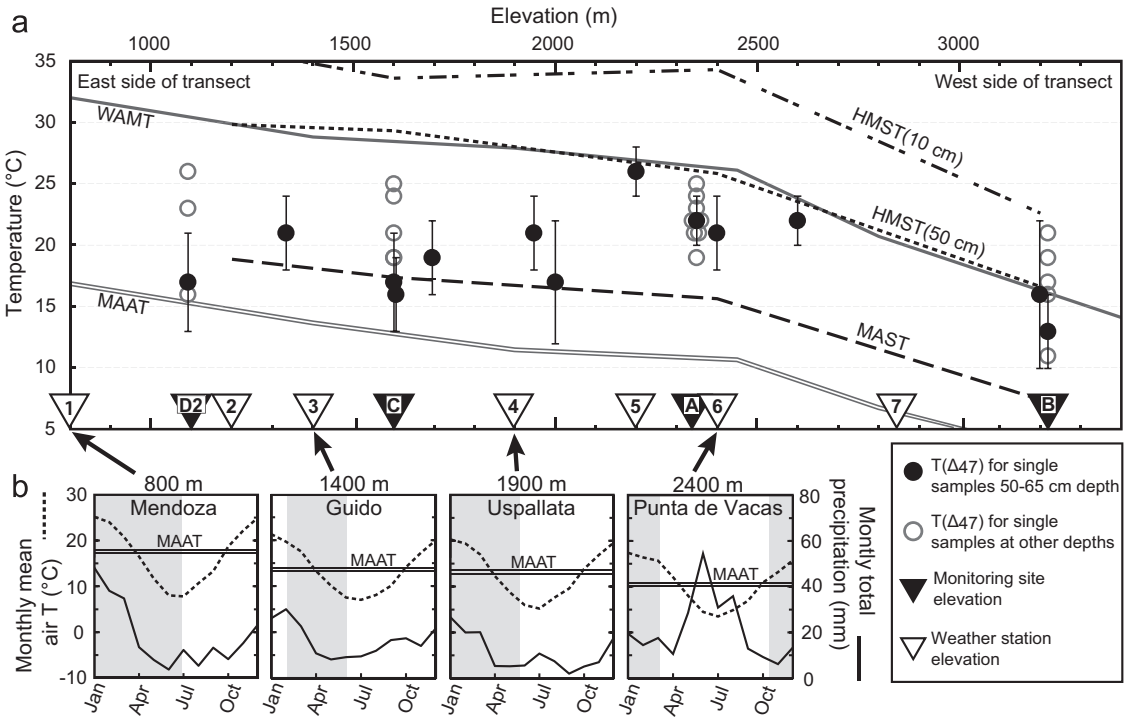

Fig. 5. (a) Air temperatures, soil temperatures, and carbonate $T(\Delta_{47})$ along the transect. At any given elevation, mean annual soil temperature (MAST, dashed line) is 3.5–5.0 °C greater than mean annual air temperature (MAAT, double gray line), hottest measured soil temperature (HMST) at 10 cm (dash-dotted line) is greater than warmest monthly mean air temperature (WAMT, solid gray line), and HMST at 50 cm (dotted line) is within 1–2 °C of WAMT. For all samples, $T(\Delta_{47})$ exceeds MAAT and ranges from MAST to hottest measured soil temperatures; note that for three of the four depth profiles, $T(\Delta_{47})$ for the 50–65 cm sample (black filled circles with 1SE error bars) is lower than the profile average (see Fig. 4). $T(\Delta_{47})$ values for samples collected at other depths are shown with open circles (error bars shown in Fig. 4). (b) MAAT (double solid line), monthly mean air temperature (dotted line), and monthly total precipitation (solid line) for weather stations 1, 3, 4, and 6. Seasonal temperature changes are in phase along the entire transect, while season of precipitation reverses between 1900 and 2200 m elevation (see also Fig. 3; weather station 5). Gray shaded boxes represent hypothesized timing of soil drying; at elevations below ~2000 m, soil drying likely occurs as precipitation decreases in the fall. At elevations greater than ~2000 m, precipitation occurs during the winter months and soil drying is likely limited to spring and summer, depending on snow melt.

for the >2000 m samples approach WAMT, suggesting warm season soil carbonate growth, results for the lower-elevation samples suggest growth during other times. Possible explanations for the relatively cooler (with respect to WAMT) $T(\Delta_{47})$ results at low elevation could include variations in aspect, shading from topography or vegetation, or soil moisture, which could make soils significantly cooler relative to WAMT during the warm summer months.

In a relatively narrow, high-relief valley such as that of the Río Mendoza, it is reasonable to suspect local aspect (i.e., slope orientation and angle) and topographic shading effects might exert a strong control on solar heating of the surface. Our sample sites are distributed across a range of valley orientations and widths that do not vary systematically with elevation. Of the monitoring sites, only the 1600 m site is located in a narrow, N–S trending portion of the Río Mendoza valley, while the other three sites occupy relatively wide E–W oriented portions of the valley. Aspect and relief vary significantly among the shallow pit sampling sites, but not systematically with elevation. Thus if aspect or topographic shading exerted a strong control on soil temperature, we would expect more scatter in the $T(\Delta_{47})$ data and instrumented pit temperatures yielding vastly different offsets with MAAT instead of the regular 3.5–5.0 °C offset for MAAT and MAST we observe (Fig. 5).

Alternatively, the observed systematic bias in $T(\Delta_{47})$ could be caused by shading from vegetation that varies systematically with elevation. Significant differences in solar radiative heating related to vegetation density (Passey et al., 2010; Quade et al., 2011, in press) and/or seasonal changes in leaf cover could dampen or amplify changes in ground surface temperature. This could be an important consideration, since vegetation cover, and, thus, shading does decrease with elevation in this region. If this shading effect leads to a significant gradient in solar radiative heating of the soil surface, we would expect low elevation soils to be relatively cooler (with respect to air WAMT) compared to higher-elevation soils (i.e., leading to a lowering of the elevation gradient in MAST). However, monitoring station data show that the offset between soil and air temperatures is constant at all elevations, ruling out this hypothesis (Fig. 5). Following similar logic we can rule out any factors, including soil moisture, that might lead to a systematic increase in the offset between MAAT and MAST, as being responsible for the lack of elevation signal in the $T(\Delta_{47})$ data.

6.2. Time dependence of soil carbonate $T(\Delta_{47})$

Since the relationship between soil and air temperatures appears straightforward, we turn to elevation-dependent differences in the timing of soil carbonate growth to account for the $T(\Delta_{47})$ results. Pedogenic carbonate develops over timescales of hundreds to thousands of years (Gile et al., 1966; Birkeland, 1999), integrating environmental conditions, including temperature, over the formation period of the carbonate. If the formation period of some soil carbonates we sampled integrates not only Holocene, but past glacial conditions, our results could be skewed towards anomalously lower temperatures. Although most carbonate samples exhibit early to middle stage I morphologies and developed in demonstrably Holocene deposits, exceptions include late stage I to stage II carbonates from the 1100 m and 1600 m sites. If these more developed samples are indeed older and integrate carbonate formed during cooler glacial periods, $T(\Delta_{47})$ in these samples should be anomalously low relative to $T(\Delta_{47})$ for

early stage I samples. Instead, $T(\Delta_{47})$ values for nearby samples with different development stage agree and remain near MAST (e.g. samples D2 (20–100) and RM1333, and samples C (10–100) and RM1695). The observation that higher elevation samples instead mimic WAMT suggests that the seasonal bias in soil carbonate formation is an important control on $T(\Delta_{47})$ and varies with elevation.

6.3. Seasonal controls on soil carbonate $T(\Delta_{47})$

Our clumped isotope results for the high elevation samples suggest a warm season bias in carbonate formation, similar to other recent studies (Breecker et al., 2009; Quade et al., 2011). However, $T(\Delta_{47})$ data for low elevation samples may instead indicate processes driving carbonate saturation during spring, fall, or other times throughout year.

A key factor that affects carbonate saturation and also varies systematically with elevation in this study region is the seasonality of precipitation (Fig. 3), and we suggest this exerts a strong control on the timing of soil carbonate formation and temperature recorded by clumped isotopes. Carbonate formation in soils is promoted by drying events, which are posited to occur following the wet season (Breecker et al., 2009). At lower elevation sites where precipitation is concentrated from late spring to early fall, soils remain moist when air and soil temperatures are significantly above MAAT and MAST. We suggest that carbonate formation occurs when soils dry in the fall and soil temperatures are closer to MAST than WAMT (Fig. 5b). The areas above 2000 m receive winter precipitation, and at the highest elevations much of this precipitation is snowfall, which leads to an influx of meltwater in the spring and early summer. As a consequence, carbonate formation in these areas is likely restricted to the summer months as the soil dries, when soil temperatures are closer to WAMT (Fig. 5b).

In our arid to semi-arid study area, soil respiration is intimately linked to precipitation, and therefore biological mediation of soil CO_2 concentrations may also play an important role in regulating soil carbonate formation. Plant roots and microbes are the primary producers of soil CO_2, modifying pCO_2 in the soil profile through changes in respiration rates. Soil microbes are known to precipitate calcite in soils (e.g. Monger et al., 1991), and plant roots can form carbonate root casts as they take up water, drying soils. In dryland environments with annual precipitation less than 600 mm, such as our study area, water availability, not temperature is the most important factor affecting biologic productivity (Austin et al., 2004). At the end of the wet season, soil respiration rates decrease and plants may efficiently dry out soils, leading to carbonate formation.

6.4. Depth controls on $T(\Delta_{47})$

Depth trends in $T(\Delta_{47})$ have the potential to provide additional insight into soil carbonate formation processes and timing. For instance, soil physics (Hillel, 1982) and our sensor data show that temperature profiles in soils are characteristic of season and vary predictably with depth (Fig. 4), so we might expect a seasonal bias in carbonate formation to be reflected in $T(\Delta_{47})$ depth trends. Although some scatter in $T(\Delta_{47})$ depth profiles is expected due to the 2–6 °C uncertainty in our clumped isotope data, average uncertainties are ~3 °C, and our sensor data indicate the difference between maximum summer soil temperatures at 10 cm and 100 cm depth ranges from 7 to 11 °C. Thus, the precision of our $T(\Delta_{47})$ results should be sufficient to resolve depth trends in carbonate formation temperature if they are present.

The $T(\Delta_{47})$ data from the monitoring sites do not show systematic trends with depth (Fig. 4). At low elevation monitoring sites we observed no systematic decrease or increase in $T(\Delta_{47})$ with depth, and $T(\Delta_{47})$ values are within 1SE of MAST in half of the samples (Fig. 4), which is generally consistent with a fall soil temperature profile and supports our hypothesis that carbonate formation occurs after the rainy summer season. At high elevation sites, the similarity of average soil $T(\Delta_{47})$ to WAMT and the fact that $T(\Delta_{47})$ values for all but one sample are significantly above MAST indicates a warm season bias in carbonate formation, which should result in a decrease in $T(\Delta_{47})$ with depth (e.g. Quade et al., in press). However, we do not observe the expected trend of cooler $T(\Delta_{47})$ with depth, and the absence of this trend may instead reflect diachronous carbonate formation with depth.

It is possible that soil carbonate formation in this area occurs more frequently near the surface than at greater depths. $T(\Delta_{47})$ values at greater depths (~75–100 cm) in three of the four monitoring pits (1100, 2400, and 3200 m) are within error of, or warmer than, maximum measured soil temperatures at 100 cm (Fig. 4). These results may suggest that soil carbonate deep in the profile formed only during drying events when soils were abnormally hot, possibly due to interannual or longer-timescale soil temperature variations over the Holocene. Based on paleoclimate records from lacustrine sediments in Chile (e.g. Lamy et al., 1999; Jenny et al., 2002) and a compilation of palynologic studies on east the side of the Andes (García et al., 1999; Markgraf, 1983; Zarate and Paez, 2002), Mancini et al. (2005) suggest that local climatic conditions varied marginally over the Holocene between slightly warmer, wetter conditions and slightly cooler, drier conditions relative to today. Although these climate shifts were minor, only modifying the geographic distribution of the same groups of steppe grasses and shrubs observed in the area today, slightly warmer, wetter conditions could result in carbonate formation at greater depths at warmer temperatures. Thus, not only seasonal variation, but variation on interannual and/or longer timescales over the Holocene may influence the frequency of carbonate-forming events and therefore $T(\Delta_{47})$-depth trends.

Alternatively, $T(\Delta_{47})$-depth patterns could reflect heterogeneity in soil properties or the stochastic nature of precipitation events. Soil carbonate formation is influenced by soil water content and its availability to organisms, which may be heterogeneous on the scale of 10–100 cm. As a consequence, localized water uptake from roots and preferential drying pathways may also influence variation in $T(\Delta_{47})$ with depth. With respect to precipitation, below 2 km elevation in our study area, precipitation occurs during austral summer in the form of sudden, spatially isolated heavy precipitation from convective storms (e.g. Prohaska, 1976). These storms result in discrete wetting events in the soil, which in arid environments can play a significant role in moderating soil respiration rates (Huxman et al., 2004; D'Odorico and Porporato, 2006). We suggest the time-integrated effect of precipitation events and soil heterogeneity on carbonate formation may contribute to the observed deviation from simple end-member predictions in our $T(\Delta_{47})$ depth profiles.

6.5. Implications for isotopic records from pedogenic carbonates

Based on our data, pedogenic carbonate $T(\Delta_{47})$ is not uniquely interpretable as WAMT, MAAT, or MAST everywhere, potentially limiting its straightforward application as a paleoclimate proxy and paleoaltimeter. Our results differ from other studies, which report $T(\Delta_{47})$ values that are closer to WAMT, challenging the universality of the hypothesis that soil carbonate growth and resulting $T(\Delta_{47})$ reflect warm-season temperatures. These results both suggest further research on the role precipitation regimes play in moderating pedogenic carbonate formation is needed to evaluate how seasonally biased carbonate formation can influence paleoenvironmental studies, and underscore the need to

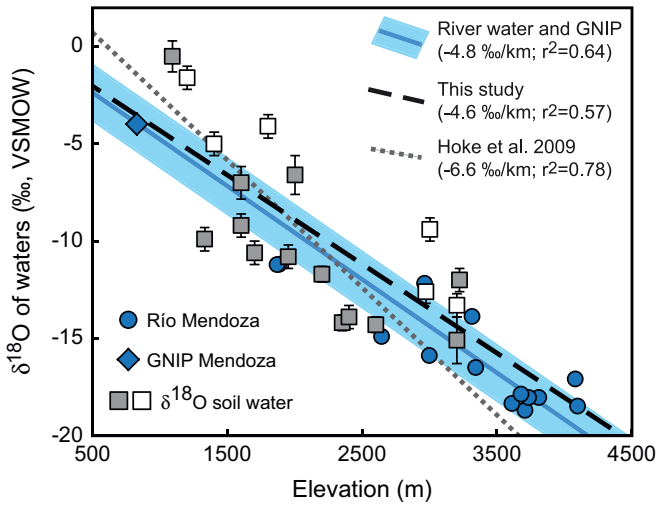

Fig. 6. Comparison of modern river water $\delta^{18}O$ values and soil water $\delta^{18}O$ values calculated from soil carbonate $\delta^{18}O$ and $T(\Delta_{47})$ for samples collected at 45–65 cm depth. Río Mendoza $\delta^{18}O$ data (blue circles) are plotted vs. mean catchment elevation and Global Network of Isotopes in Precipitation (GNIP) station data (blue diamond) after Hoke et al. (2009). Calculated soil water $\delta^{18}O$ values for samples from this study (gray squares with 1SE error bars) are plotted along with soil water $\delta^{18}O$ values for samples from Hoke et al. (2009) that were not analyzed using clumped isotope thermometry (white squares with 1SE error bars). The latter were calculated from published carbonate $\delta^{18}O$ values by estimating the carbonate formation temperature based on $T(\Delta_{47})$ for nearby samples at similar elevation (samples and temperature estimates: MODS 07-01, 17 °C; MODS 07-02, 16 °C; MODS 07-04, 19 °C; MODS 07-08a,b, 15 °C; MODS 07-09, 15 °C; MODS 07-03, 16 °C; all assigned +/−3 °C nominal 1SE uncertainty). Linear regression lines are shown for Río Mendoza and GNIP $\delta^{18}O$ data (blue line; shaded blue area shows 1σ uncertainty), soil water calculated using $T(\Delta_{47})$ for this study (black dashed line), and soil water calculated using MAAT for all samples (gray dotted line; from Hoke et al., 2009). (For interpretation of the references to color in this figure legend, the reader is referred to the web version of this article.)

independently constrain carbonate formation temperatures when estimating the $\delta^{18}O$ values of soil waters.

To illustrate the importance of accurately constraining carbonate formation temperatures, we estimate soil water $\delta^{18}O$ values by using $T(\Delta_{47})$ of our samples to calculate the temperature-dependent water–calcite fractionation factor, and compare these values to both $\delta^{18}O$ values of modern river waters and to previous estimates of soil water $\delta^{18}O$ values calculated using MAAT for all samples (Fig. 6). Using $T(\Delta_{47})$ to calculate soil water $\delta^{18}O$ values produces a lapse rate of −4.6‰/km, which is remarkably similar to the river water $\delta^{18}O$ lapse rate of −4.8‰/km reported by Hoke et al. (2009). When MAAT is used to estimate soil water $\delta^{18}O$ values, the resulting $\delta^{18}O$ lapse rate is −6.6‰/km, considerably steeper than that of river water and potentially leading to estimates of surface water $\delta^{18}O$ values in error by up to 3‰. This error corresponds to elevation overestimates of 0.6 km in the Central Andes, where the $\delta^{18}O$ value of precipitation-elevation gradient is steep (~5‰/km; Hoke et al., 2011), or >1 km in areas with average isotopic gradients (2.8‰/km; Poage and Chamberlain, 2001).

7. Conclusions

The reversal of wet season across the eastern flank of the central Andes creates an opportunity to investigate the influence of environmental factors most commonly identified as drivers of carbonate formation. In this region, we find carbonate formation temperature does not correspond to a simple climate metric such as MAAT or WAMT. We suggest the change in precipitation regime across the study area controls the timing of carbonate formation throughout the year, and this timing ultimately determines the soil temperatures at which the carbonates form. A consideration that cannot be addressed in a study region in which precipitation season is reversed from low to high elevation is the effect at high elevations of snowmelt on delaying the onset of soil drying that drives carbonate formation in the soil profile. Such an effect may create an elevation dependent seasonal transition in soil drying that may be endemic to elevated terrain regions. This outstanding question could be addressed by research along a similar elevation transect with a single moisture source and uniform wet season. Such a study would serve to test our hypothesis that precipitation season is a dominant control on carbonate formation temperature and tease out the effects of other environmental factors that can influence offsets between soil and air temperatures such as solar heating of the ground surface, vegetation, and insulating snow cover.

In this study region, $T(\Delta_{47})$ values from lower elevations are indistinguishable from those at higher elevations, making it impossible to reconstruct a mean annual air- or soil-temperature-elevation gradient. Although this seasonal precipitation bias may be limited to unique situations such as the lee side of relatively narrow linear mountain ranges where the potential for spill over precipitation is high (e.g. the Andes outside of the Altiplano-Puna and the Sierra Nevada of California), this effect must be carefully considered in any paleoenvironmental interpretations based on pedogenic carbonate formation temperatures. Nevertheless, clumped isotope thermometry can substantially improve estimates of elevation using calculated soil water $\delta^{18}O$-elevation gradients. The use of clumped isotope thermometry to constrain carbonate formation temperatures needed to accurately calculate soil water $\delta^{18}O$ values from pedogenic carbonate need not be limited to paleoelevation studies and, in conjunction with other environmental proxies such as $\delta^{13}C$ values, biomarkers, and paleobotany, should be broadly applicable as a paleoenvironmental proxy in all terrestrial settings where pedogenic carbonate occurs.

Acknowledgments

We thank Mariana Bonich and Maximiliano Viale for assistance in the collection of field data and John Eiler and Nami Kitchen for generous lab access and assistance at Caltech. Dan Breecker and Jay Quade are acknowledged for stimulating discussion as our work progressed, and we thank two anonymous reviewers and Editor Jean Lynch-Stieglitz for helpful comments that improved the paper. NAP was supported by the Goodspeed and Misch Fellowships in the Department of Earth and Space Sciences at the University of Washington. GDH was supported by the NSF award No. OISE-0601957.

Appendix A. Supporting information

Supplementary data associated with this article can be found in the online version at http://dx.doi.org/10.1016/j.epsl.2012.10.024.

References

Amundson, R., Chadwick, O., Kendall, C., Wang, Y., DeNiro, M., 1996. Isotopic evidence for shifts in atmospheric circulation patterns during the late Quaternary in mid-North America. Geology 24, 23–26.

Austin, A.T., Yahdjian, L., Stark, J.M., Belnap, J., Porporato, A., Norton, U., Ravetta, D.A., Schaeffer, S.M., 2004. Water pulses and biogeochemical cycles in arid and semiarid ecosystems. Oecologia 141, 221–235.

Barros, V.R., Castañeda, M.E., Doyle, M., 1996. Recent precipitation trends in southern South America to the east of the Andes: an indication of a mode of climatic variability. in: Rosa, L.P., Santos, M.A. (Eds.), Greenhouse Gas Emission

Under Developing Countries Point of View. COPPE (Alberto Luiz Coimbra Institute and Graduate School of Research and Engineering), Rio de Janeiro, pp. 41–67.
Bartlett, M.G., Chapman, D.S., Harris, R.N., 2006. A decade of ground-air temperature tracking at Emigrant Pass Observatory, Utah. J. Climate 19, 3722–3731.
Birkeland, P.W., 1999. Soils and Geomorphology, third ed. Oxford University Press, New York.
Breecker, D.O., Sharp, Z.D., McFadden, L.D., 2009. Seasonal bias in the formation and stable isotopic composition of pedogenic carbonate in modern soils from central New Mexico, USA. Geol. Soc. Am. Bull. 121, 630–640.
Cavagnaro, J.B., 1988. Distribution of C_3 and C_4 grasses at different altitudes in a temperate arid region of Argentina. Oecologia 76, 273–277.
Cerling, T.E., Quade, J., 1993. Stable carbon and oxygen isotopes in soil carbonates. in: Swart, P.K., et al. (Eds.), Climate Change in Continental Isotopic Records, Geophysical Monograph Series, vol. 78. AGU, Washington, DC, pp. 217–231.
Cerling, T.E., Wynn, J.G., Andanje, S.A., Bird, M.I., Korir, D.K., Levin, N.E., Mace, W., Macharia, A.N., Quade, J., Remien, C.H., 2011. Woody cover and hominin environments in the past 6 million years. Nature 476, 51–56.
Coops, N.C., Waring, R.H., Moncrieff, J., 2000. Estimating mean monthly incident solar radiation on horizontal and inclined slopes from mean monthly temperatures extremes. Int. J. Biometeorol. 44, 204–211.
Cristallini, E.O., Ramos, V.A., 2000. Thick-skinned and thin-skinned thrusting in the La Ramada fold and thrust belt: crustal evolution of the high Andes of San Juan, Argentina (32°SL). Tectonophysics 317, 205–235.
D'Odorico, P., Porporato, A. (Eds.), 2006. Soil moisture dynamics in water-limited ecosystems, Dryland Ecohydrology. Springer, Netherlands pp. 31–46.
Eiler, J.M., 2007. "Clumped-isotope" geochemistry—the study of naturally-occurring, multiply-substituted isotopologues. Earth Planet. Sci. Lett. 262, 309–327.
Eiler, J.M., 2011. Paleoclimate reconstructions using carbonate clumped isotope thermometry. Q. Sci. Rev. 30, 3575–3588.
Eiler, J.M., Schauble, E., 2004. $^{18}O^{13}C^{16}O$ in Earth's atmosphere. Geochim. Cosmochim. Acta 68, 4767–4777.
Espizúa, L.E., Bigazzi, G., 1998. Fission-track dating of the Punta de Vacas glaciation in the Rio Mendoza valley, Argentina. Q. Sci. Rev. 17, 755–760.
Espizúa, L.E., 1999. Chronology of late Pleistocene glacier advances in the Rio Mendoza Valley, Argentina. Global Planet. Change 22, 193–200.
Espizúa, L.E., 2002. Quaternary glaciations in the Rio Mendoza Valley, Argentine Andes. Q. Geol., 111–115.
Espizúa, L.E., 2003. Glaciacones Cuaternarias en el valle del Río Mendoza, Andes Argentinos, IANIGLA. 30 Años de Investigación básica y aplicada en Ciencias Ambientales, Mendoza, IANIGLA-CONICET, p. 111–115.
Flanagan, L.B., Varney, G.T., 1995. Influence of vegetation and soil CO_2 exchange on the concentration and stable oxygen isotope ratio of atmospheric CO_2 within a Pinus resinosa canopy. Oecologia 101, 37–44.
Flerchinger, G.N., Pierson, F.B., 1997. Modelling plant canopy effects on variability of soil temperature and water: model calibration and validation. J. Arid Environ. 35, 641–653.
García, A., Zárate, M., Paez, M.M., 1999. The Pleistocene/Holocene transition and human occupation in the Central Andes of Argentina: Agua de la Cueva locality. Q. Int. 53–54, 43–52.
Garzione, C.N., Dettman, D.L., Quade, J., DeCelles, P.G., Butler, R.F., 2000. High times on the Tibetan Plateau: paleoelevation of the Thakkhola graben, Nepal. Geology 28, 339–342.
Ghosh, P., Adkins, J., Affek, H., Balta, B., Guo, W., Schauble, E., Schrag, D., Eiler, J., 2006a. ^{13}C–^{18}O bonds in carbonate minerals: a new kind of paleothermometer. Geochim. Cosmochim. Acta 70, 1439–1456.
Ghosh, P., Garzione, C.N., Eiler, J.M., 2006b. Rapid uplift of the Altiplano revealed through ^{13}C–^{18}O bonds in paleosol carbonates. Science 311, 511–515.
Gile, L.H., Peterson, F.F., Grossman, R.B., 1966. Morphological and genetic sequences of carbonate accumulation in desert soils. Soil Sci. 101, 347–360.
Gonfiantini, R., Roche, M.-A., Olivry, J.-C., Fontes, J.-C., Zuppi, G.M., 2001. The altitude effect on the isotopic composition of tropical rains. Chem. Geol. 181, 147–167.
Hillel, D., 1982. Introduction to Soil Physics. Academic Press, New York.
Hoke, G.D., Garzione, C.N., Araneo, D.C., Latorre, C., Strecker, M.R., Williams, K.J., 2009. The stable isotope altimeter: do quaternary pedogenic carbonates predict modern elevations? Geology 37, 1015–1018.
Hoke, G.D., Aranibar, J.N., Viale, M., Araneo, D.C., Llano, C., 2011. Isotopic Characterization of Mountain Precipitation Along the Eastern Flank of the Andes Between 32.5–35°S, 2011 AGU Fall Meeting, San Francisco.
Huntington, K.W., Eiler, J.M., Affek, H.P., Guo, W., Bonifacie, M., Yeung, L.Y., Thiagarajan, N., Passey, B., Tripati, A., Daeron, M., Came, R., 2009. Methods and limitations of 'clumped' CO_2 isotope (Δ_{47}) analysis by gas-source isotope ratio mass spectrometry. J. Mass Spectrom. 44, 1318–1329.
Huntington, K.W., Wernicke, B.P., Eiler, J.M., 2010. Influence of climate change and uplift on Colorado Plateau paleotemperatures from carbonate 'clumped isotope' thermometry. Tectonics 29, TC3005, http://dx.doi.org/10.1029/2009TC002449.
Huxman, T.E., Snyder, K.A., Tissue, D., Leffler, A.J., Ogle, K., Pockman, W.T., Sandquist, D.R., Potts, D.L., Schwinning, S., 2004. Precipitation pulses and carbon fluxes in semiarid and arid ecosystems. Oecologia 141, 254–268 http://dx.doi.org/10.1007/s00442-004-1682-4.
Jenny, B., Valero-Garces, B., Villa-Martinez, R., Urrutia, R., Geyh, M., Veit, H., 2002. Early to mid-Holocene aridity in central Chile and the southern Westerlies: the Laguna Aculeo record (34 degrees S). Q. Res. 58, 160–170.
Jordan, T.E., Isacks, B.L., Allmendinger, R.W., Brewer, J.O.N.A., Ramos, A., Ando, C.J., 1983. Andean tectonics related to geometry of subducted Nazca plate Andean tectonics related to geometry of subducted Nazca plate. Geol. Soc. Am. Bull. 94, 341–361.
Kim, S.-T., O'Neil, J.R., 1997. Equilibrium and nonequilibrium oxygen isotope effects in synthetic carbonates. Geochim. Cosmochim. Acta 61, 3461–3475.
Lamy, F., Hebbeln, D., Wefer, G., 1999. High-resolution marine record of climatic change in mid-latitude Chile during the last 28,000 years based on terrigenous sediment parameters. Q. Res. 51, 83–93.
Mancini, M., Paez, M., Prieto, A., Stutz, S., Tonello, M., Vilanova, I., 2005. Mid-Holocene climatic variability reconstruction from pollen records (32 degrees-52 degrees S Argentina). Q. Int., 47–59.
Markgraf, V., 1983. Late and Postglacial vegetational and paleoclimatic changes in subantarctic, temperate, and arid environments in Argentina. Palynology 7, 43–70.
Monger, H.C., Wilding, L.P., 2006. Inorganic carbon: composition and formation. In: Lal, R. (Ed.), Encyclopedia of Soil Science. Taylor & Francis, New York pp. 886–889.
Monger, H.C., Daugherty, L.A., Lindemann, W.C., Liddell, C.M., 1991. Microbial precipitation of pedogenic calcite. Geology 19, 997–1000.
Moreiras, S.M., 2010. Geomorphological evolution of the Mendoza River Valley. In: del Papa, C., Astini, R. (Eds.), Field Excursion Guidebook, 18th International Sedimentological Congress, Mendoza, Argentina. FE-B2, pp. 1–21.
Moreiras, S.M., 2011. Clustering of Pleistocene rock avalanches in the Central Andes (Mendoza, Argentina). in: Salfity, J.A., Marquillas, R.A. (Eds.), Cenozoic Geology of the Central Andes of Argentina. SCS Publisher, Salta, pp. 265–282.
Passey, B.H., Levin, N.E., Cerling, T.E., Brown, F.H., Eiler, J.M., 2010. High-temperature environments of human evolution in East Africa based on bond ordering in paleosol carbonates. Proc. Nat. Acad. Sci. USA 107, 11245–11249.
Pereyra, F.X., 1996. Geomorfología. In: Ramos, V.A. (Ed.) Geología de la Región del Aconcagua, Provincias de San Juan y Mendoza. vol. 24. Subsecretaria de Minería de la Nación, Dirección Nacional del Servicio Geológico, Anales, pp. 423–446.
Poage, M.A., Chamberlain, C.P., 2001. Empirical relationships between elevation and the stable isotope composition of precipitation and surface waters: considerations for studies of paleoelevation change. Am. J. Sci. 301, 1–15.
Polanski, J., 1963. Estratigrafía, neotectonica y geomorfología del Pleistoceno pedemontano entre los ríos Diamante y Mendoza, provincia de Mendoza. Rev. Asoc. Geol. Argen. 17, 127–349.
Prohaska, F., 1976. The climate of Argentina, Paraguay and Uruguay. in: Schwerdtfeger, W. (Ed.), Climate of Central and South America. Elsevier, Amsterdam, pp. 13–73.
Quade, J., Breecker, D.O., Daëron, M., Eiler, J., 2011. The paleoaltimetry of Tibet: an isotopic perspective. Am. J. Sci. 311, 77–115.
Quade, J., Cerling, T.E., Bowman, J.R., 1989a. Systematic variations in the carbon and oxygen isotopic composition of pedogenic carbonate along elevation transects in the southern Great Basin, United States. Geol. Soc. Am. Bull. 101, 464–475.
Quade, J., Garzione, C., Eiler, J., 2007. Paleoelevation reconstruction using pedogenic carbonates. in: Kohn, M. (Ed.), Paleoaltimetry: Geochemical And Thermodynamic Approaches, vol. 66. Reviews in Mineralogy and Geochemistry, pp. 53–88.
Quade, J., Cerling, T.E., Bowman, J., 1989b. Development of Asian monsoon revealed by marked ecological shift during the latest Miocene in Northern Pakistan. Nature 342, 163–166.
Quade, J., Eiler, J., Daeron, M., Breecker, D. The Clumped Isotope Geothermometer in Soil and Paleosol Carbonate. Geochimica et Cosmochimica Acta, in press.
Retallack, G.J., 2005. Pedogenic carbonate proxies for amount and seasonality of precipitation in paleosols. Geology 33, 333–336.
Retallack, G.J., 2009. Refining a pedogenic-carbonate CO_2 paleobarometer to quantify a middle Miocene greenhouse spike. Palaeogeogr. Palaeoclimatol. Palaeoecol. 281, 57–65.
Rowley, D.B., Currie, B.S., 2006. Palaeo-altimetry of the late Eocene to Miocene Lunpola basin, central Tibet. Nature 439, 677–681.
Rowley, D.B., Pierrehumbert, R.T., Currie, B.S., 2001. A new approach to stable isotope-based paleoaltimetry: implications for paleoaltimetry and paleohypsometry of the High Himalaya since the Late Miocene. Earth Planet. Sci. Lett. 5836, 1–17.
Saavedra, N., Foppiano, A.J., 1992. Monthly mean pressure model for Chile. Int. J. Climatol. 12, 469–480.
Sheldon, N.D., Tabor, N.J., 2009. Quantitative paleoenvironmental and paleoclimatic reconstruction using paleosols. Earth Sci. Rev. 95, 1–52.
Viale, M., Nuñez, M.N., 2011. Climatology of winter orographic precipitation over the subtropical Central Andes and associated synoptic and regional characteristics. J. Hydrometeorol. 12, 481–507.
Wood, W.W., Petraitis, M.J., 1984. Origin and distribution of carbon dioxide in the unsaturated zone of the southern high plains of Texas. Water Resour. Res. 20, 1193–1208.
Zarate, M., Paez, M.M., 2002. Los Paleoambientes del Pleistoceno-Holoceno en la cuenca del arroyo La Estacada, Mendoza. in: Trombotto, D., Villalba, R. (Eds.), IANIGLA, 30 años de Investigación Básica y Aplicada en Ciencias Ambientales. Institutio Argentino de Nivologia, Glaciologia y Ciencias Ambientales, IANIGLA, Mendoza, Argentina, pp. 117–121.